Journal Name

COMMUNICATION

**Supporting Information**

# Identifying the origin and contribution of the pseudocapacitive sodium ion storage in tungsten disulphide nanosheets for the application of sodium-ion capacitors

Chunxia Ding,*[b] Yaping Tao,[c] Deming Tan,[d] Yin Zhang,[a] Faxing Wang,[d] and Feng Yu*[a]

[a.] School of Chemistry, Physics and Mechanical Engineering, Science and Engineering Faculty, Queensland University of Technology, Brisbane, Australia. Email: feng.yu@hdr.qut.edu.au

[b.] College of Science, Hunan Agricultural University, Changsha, Hunan 410128, China. Email: dcxxys@hunau.edu.cn

[c.] College of Physics and Electronic Information, Luoyang Normal University, Luoyang 471022, China.

[d.] Department of Chemistry and Food Chemistry, Technische Universität Dresden, 01062 Dresden, Germany. Email: faxing.wang@tu-dresden.de.

# Supplementary Figures

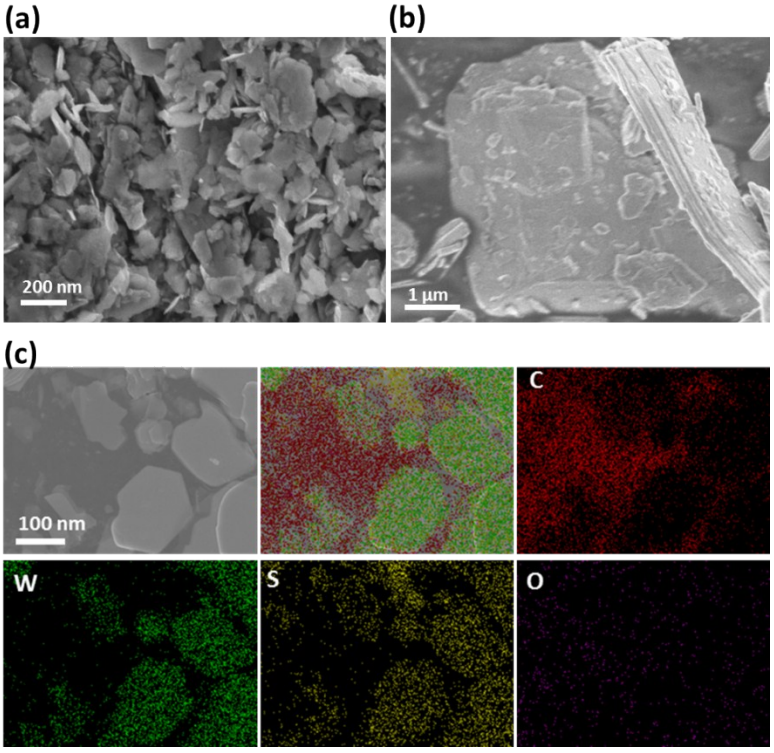


**Supplementary Figure S1**. (a) SEM images of the (a) $WS_2$ nanosheets and (b) bulk $WS_2$. (c) The corresponding elemental mapping images of the $WS_2$ nanosheets.

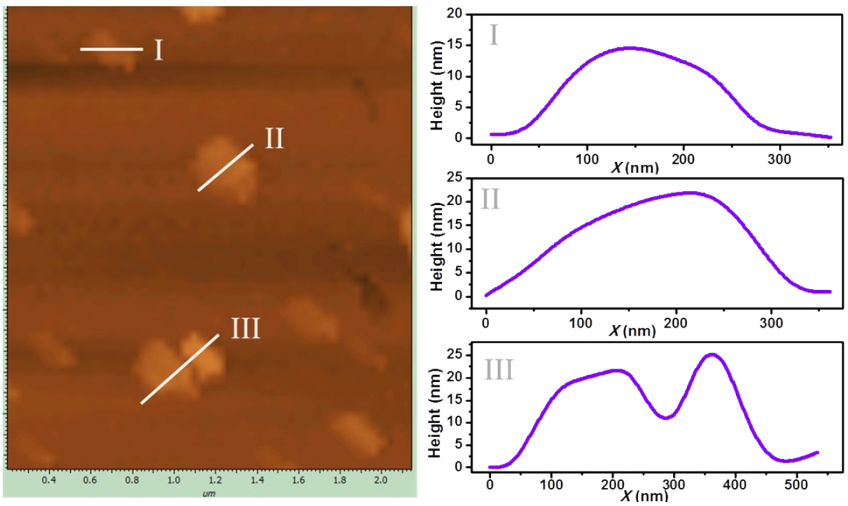


**Supplementary Figure S2**. The atomic force microscopy (AFM) image of the $WS_2$ sample and the corresponding height profile.

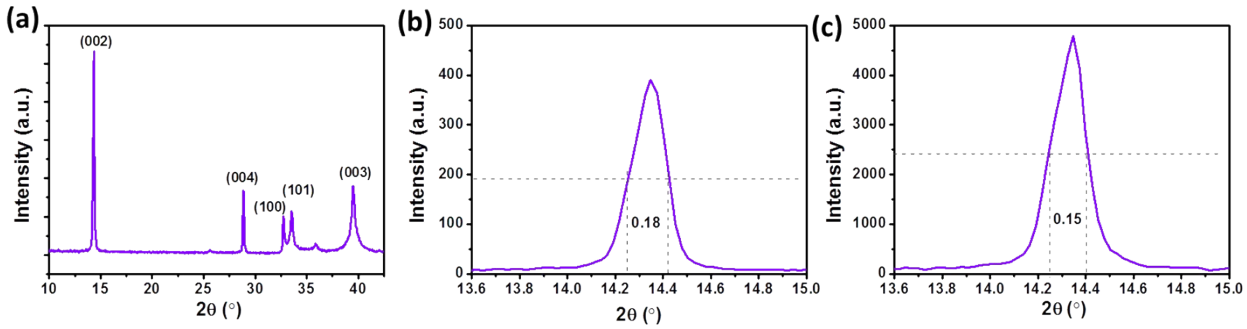


**Supplementary Figure S3**. (a) The XRD pattern of the $WS_2$ nanosheets. The full width at half maximum (FWHM) of (002) peak for (b) the $WS_2$ nanosheets and (c) bulk $WS_2$. Except for the slightly different FWHM and intensity of (002) peak, there are almost no big differences between our $WS_2$ nanosheets (with the thicknesses of 20-30 layers) and the bulk $WS_2$. This applies to many previous reported $WS_2$ nanosheets (with the thickness of >10 layers) as well.[1–4]

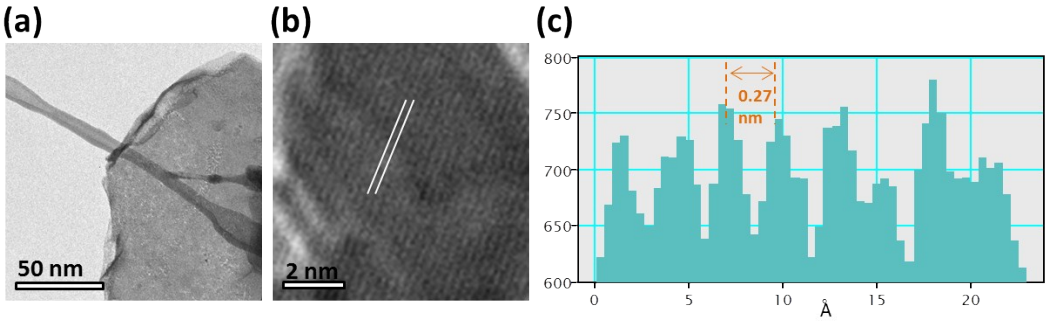


**Supplementary Figure S4**. (a, b) TEM images and (c) the corresponding lattice spacing of the $WS_2$ nanosheets.

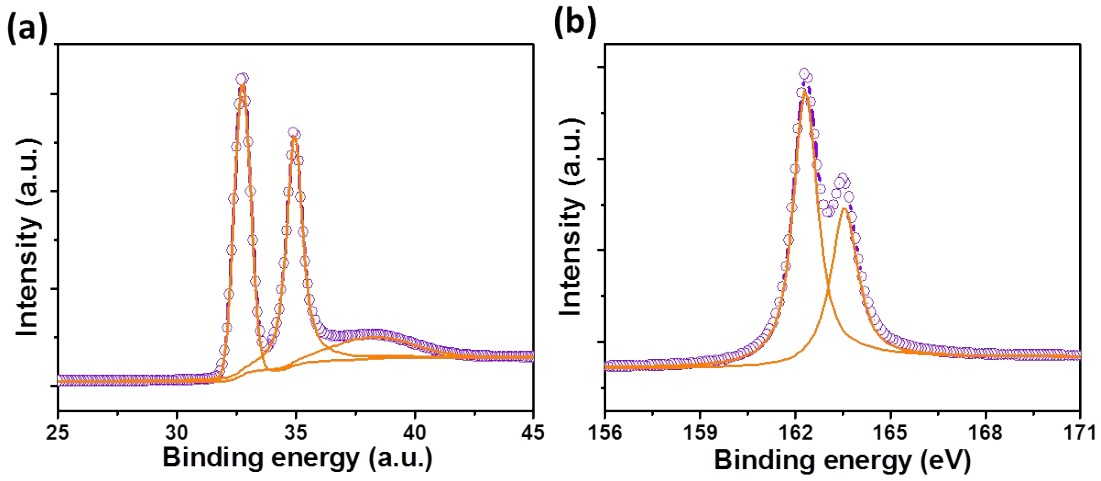


**Supplementary Figure S5**. The XPS spectrum of (a) W 4f and (b) S 2p for the $WS_2$ nanosheets.

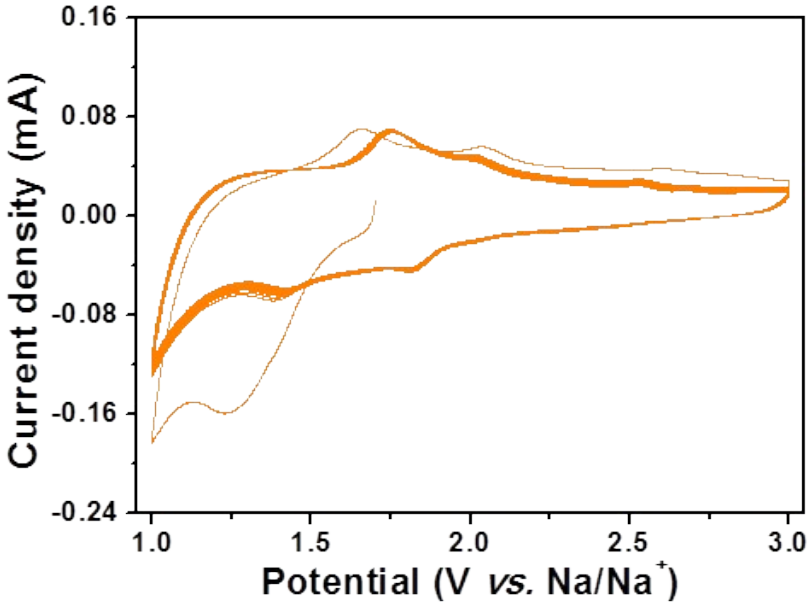


**Supplementary Figure S6**. The CV curves of the electrode based on $WS_2$ nanosheets at a sweep rate of 3 mV $s^{-1}$.

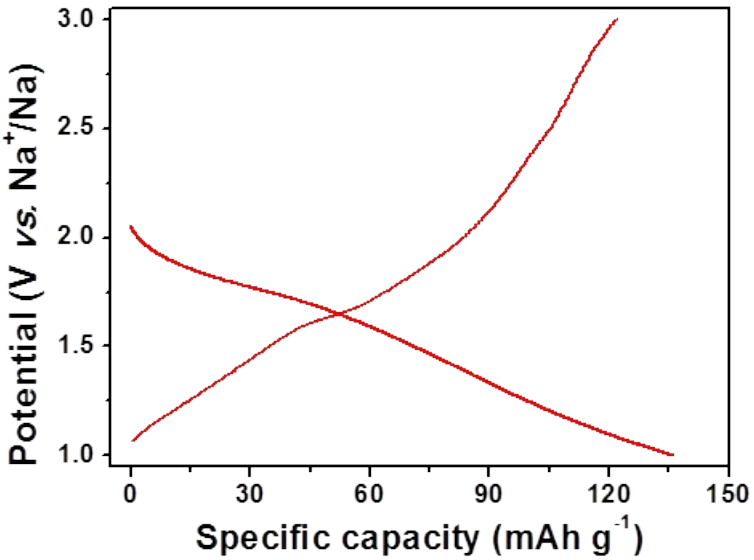


**Supplementary Figure S7**. The initial charge/discharge curves of the electrode based on $WS_2$ nanosheets at a current density of 0.1 A $g^{-1}$.

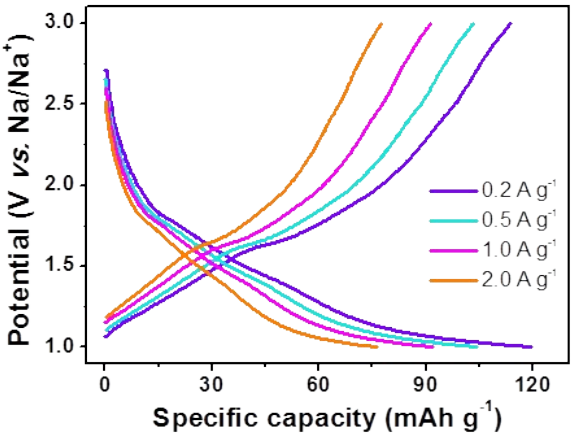


**Supplementary Figure S8**. The rate capability of the electrode based on $WS_2$ nanosheets.

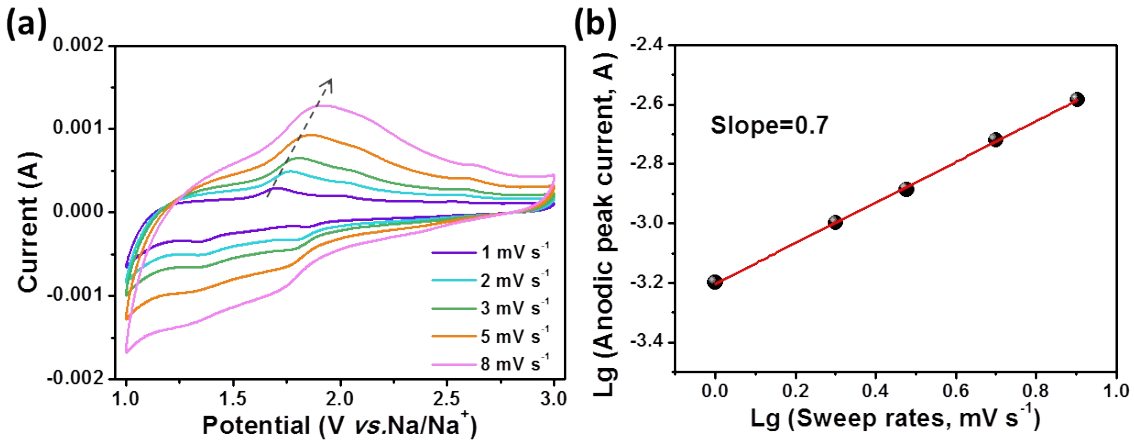


**Supplementary Figure S9**. The The CV curves of the electrode based on the $WS_2$ nanosheets at various sweep rates. (b) The determination of the *b*-value at cathodic peak regimes. The value of *b* can be determined from the slope of log (peak current) versus log (sweep rate) as following the equation of $i = av^b$, in which *a* and *b* are constants. The *b* value of 0.5 indicates diffusion-controlled charge storage and the value of 1 suggests a capacitive (or pseudocapacitive) charge-storage mechanism. Here the *b* value calculated at the anodic peak regimes was estimated to be 0.7, suggesting the combination of a capacitance-controlled current and a diffusion-controlled current. In this case, the current can be separated into capacitive ($k_1v$) contribution and diffusion-controlled contribution ($k_2v^{1/2}$) as follows: $i = k_1v + k_2v^{1/2}$. Then, the $k_1$ and $k_2$ contents at various potentials can be determined by plotting $i/v^{1/2}$ versus $v^{1/2}$.[5–8]

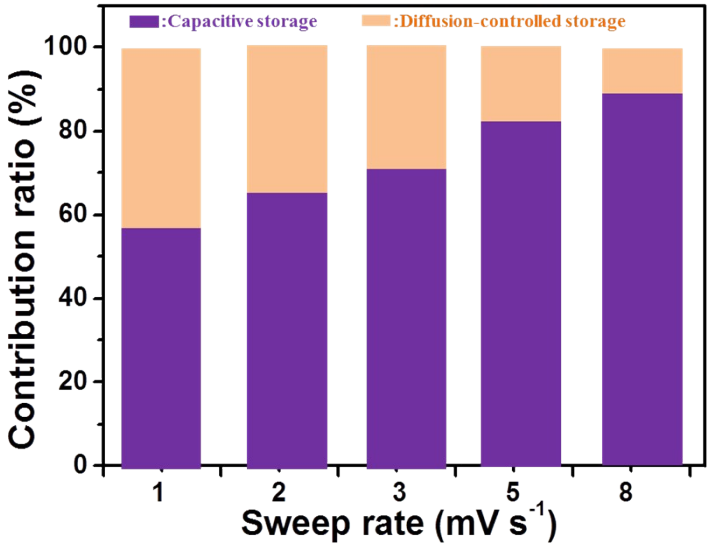


**Supplementary Figure S10**. Contribution ratios of capacitances from the surface-controlled charge storage and diffusion-limited charge storage for the electrode based on $WS_2$ nanosheets at various sweep rates.

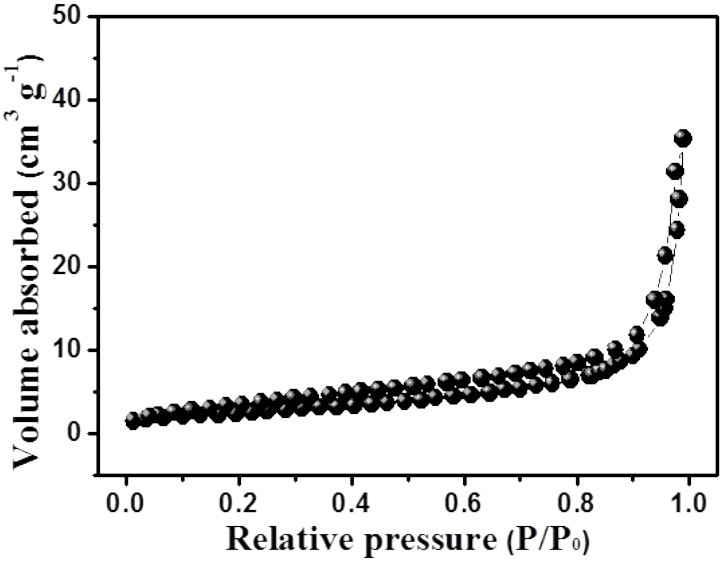


**Supplementary Figure S11**. The $N_2$ adsorption-desorption isotherm of the for the $WS_2$ nanosheets with a specific surface area of 28 $m^2$ $g^{-1}$.

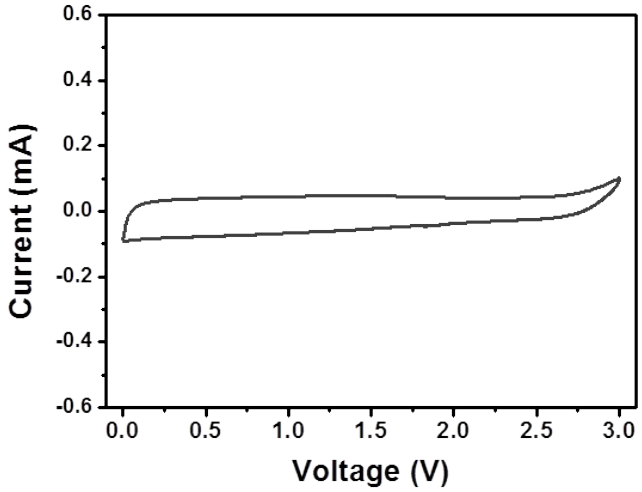


**Supplementary Figure S12**. The electrical-double-layer typed capacitive test in a standard ionic liquid electrolyte (EMI-$BF_4$) [9] for a symmetrical supercapacitor based on the $WS_2$ nanosheets as electrodes. The specific capacitance was calculated to be about 1.95 F $g^{-1}$. This EDLC contribution is low since the specific capacitance is proportional to the specific surface area to a certain extent.[10]

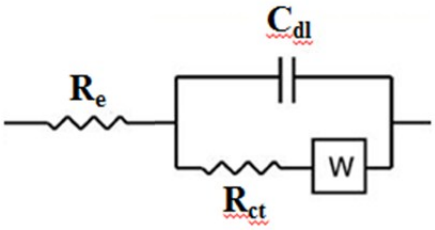


**Supplementary Figure S13**. The used equivalent circuit for fitting impedance spectra of the electrode based on the $WS_2$ nanosheets in the potential range of 1−3V *vs.* $Na/Na^+$.

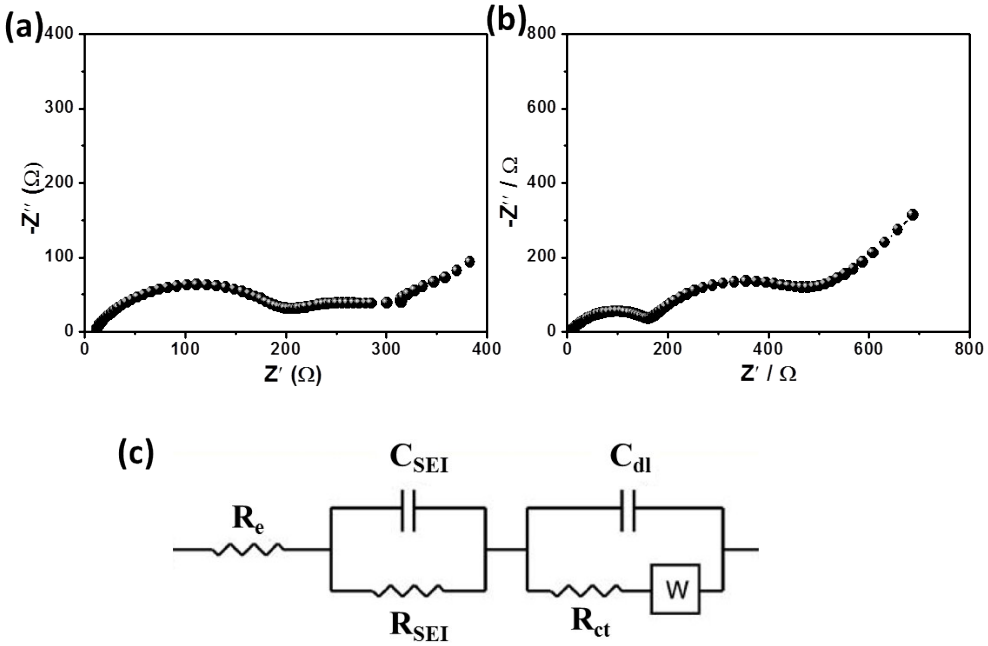


**Supplementary Figure S14**. Nyquist plots of the electrode based on the $WS_2$ nanosheets was discharged to the (a) 0.5 V and (b) 0.1 V *vs.* $Na/Na^+$. (c) The used equivalent circuit for fitting impedance spectra.

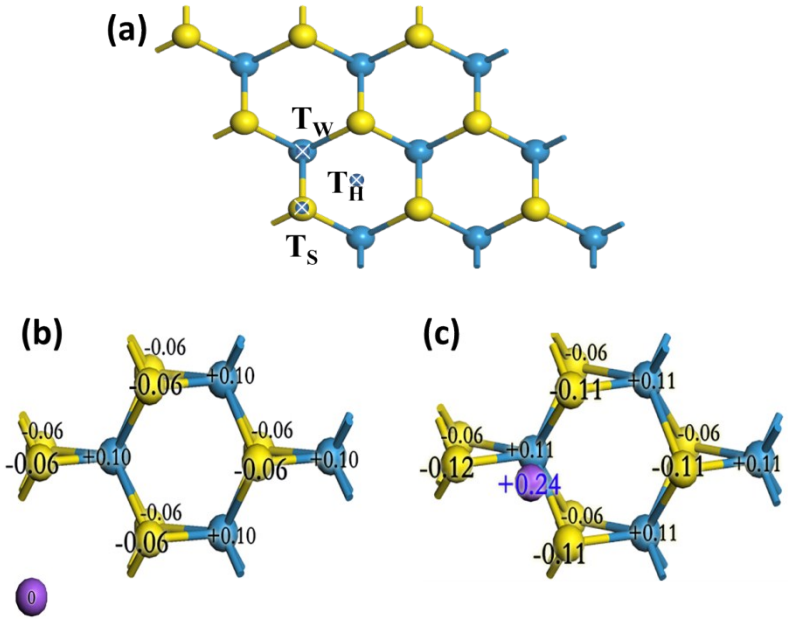


**Supplementary Figure S15**. (a) Schematic illustration of the different site for surface Na ion storage. Hirshfeld charges distribution (b) before and (c) after Na adsorption. The yellow, blue and purple spheres are the S, W and Na atom, respectively.

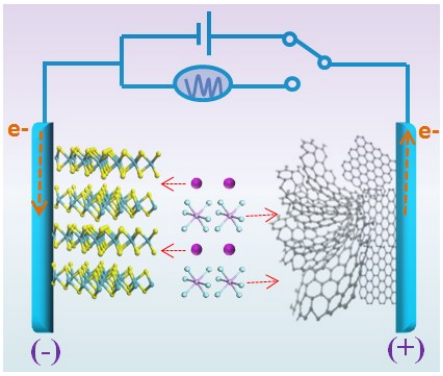


**Supplementary Figure S16**. Schematic illustration of the fabricated Na-ion capacitor based on the $WS_2$ nanosheets as the anode.

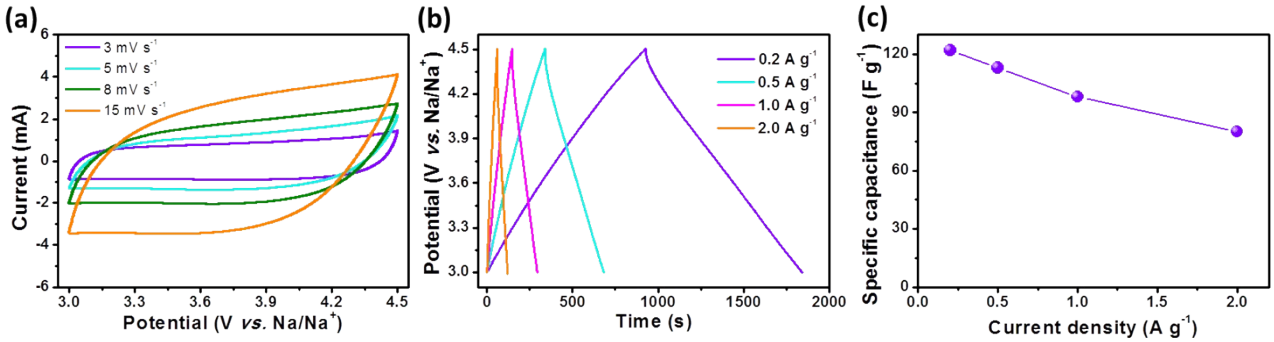


**Supplementary Figure S17**. The electrochemical behaviours of the used cathode for the $WS_2$ based Na ion capacitor. (a) The CV curves at various sweep rates. (b) Galvanostatic charge/discharge profiles and (c) specific capacitances at various current densities. The mass ratio of the used cathode and $WS_2$ anode was obtained according to the following equation: $Q_+ = Q_- = m_+ \times U_+ \times C_+ = m_- \times U_- \times C_-$, where Q is the capacity, U is the potential range, m is the mass of active electrode, and subscripts stand for the cathode and anode, respectively.[11,12]

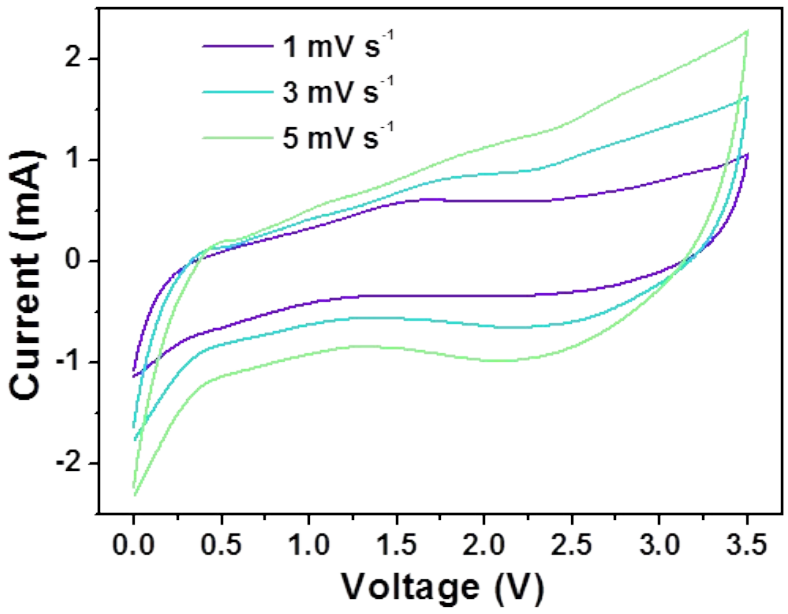


**Supplementary Figure S18**. The CV curves of the fabricated Na-ion capacitor based on $WS_2$ nanosheets as the anode at various sweep rates

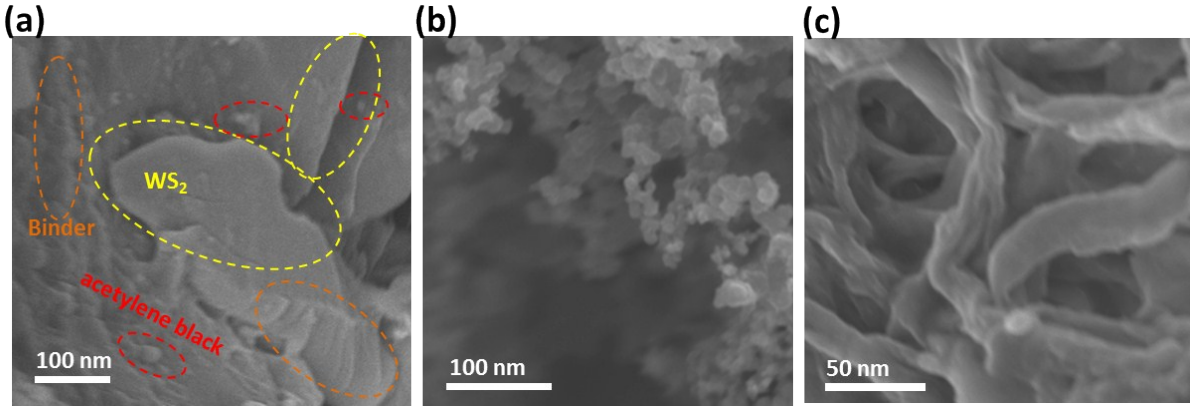


**Supplementary Figure S19**. The SEM image of (a) the $WS_2$ anode for the Na-ion capacitor after 6000 cycles, (b) the acetylene back and (c) the binder

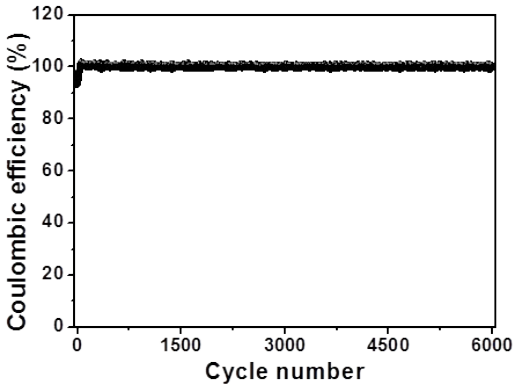


**Supplementary Figure S20**. The coulombic efficiencies of the fabricated Na-ion capacitor during the cycling process.

**Supplementary Table S1.** Hirshfeld charges distribution before and after Na adsorption.

| | $WS_2$ | T_W |
|---|---|---|
| $Na_1$ | | 0.23 |
| $S_1$ | -0.06 | -0.06 |
| $S_2$ | -0.06 | -0.11 |
| $S_3$ | -0.06 | -0.06 |
| $S_4$ | -0.06 | -0.1 |
| $S_5$ | -0.06 | -0.06 |
| $S_6$ | -0.06 | -0.11 |
| $S_7$ | -0.06 | -0.06 |
| $S_8$ | -0.06 | -0.11 |
| $W_1$ | 0.1 | 0.11 |
| $W_2$ | 0.1 | 0.11 |
| $W_3$ | 0.1 | 0.11 |
| $W_4$ | 0.1 | 0.11 |

**References**

1 X. Mao, Y. Xu, Q. Xue, W. Wang and D. Gao, *Nanoscale Res. Lett.*, 2013, **8**, 430–435.

2 Y. Hongjian, Y. Yong, L. Jianghao, M. Peiyan, W. Yucheng, Z. Fan and F. Zhengyi, *J. Mater. Chem. A*, 2015, **3**, 19439–19444.

3 Q. Liu, X. Li, Z. Xiao, Y. Zhou, H. Chen, A. Khalil, T. Xiang, J. Xu, W. Chu, X. Wu, J. Yang, C. Wang, Y. Xiong, C. Jin, P. M. Ajayan and L. Song, *Adv. Mater.*, 2015, **27**, 4837–4844.

4 D. Zheng, Y. P. Wu, Z. Y. Li and Z. B. Cai, *RSC Adv.*, 2017, **7**, 14060–14068.

5 T. Brezesinski, J. Wang, S. H. Tolbert and B. Dunn, *Nat. Mater.*, 2010, **9**, 146–151.

6 V. Augustyn, J. Come, M. A. Lowe, J. W. Kim, P. L. Taberna, S. H. Tolbert, H. D. Abruna, P. Simon and B. Dunn, *Nat. Mater.*, 2013, **12**, 518–522.

7 H. S. Kim, J. B. Cook, H. Lin, J. S. Ko, S. H. Tolbert, V. Ozolins and B. Dunn, *Nat. Mater.*, 2017, **16**, 454–460.

8 F. Wang, X. Wu, X. Yuan, Z. Liu, Y. Zhang, L. Fu, Y. Zhu, Q. Zhou, Y. Wu and W. Huang, *Chem. Soc. Rev.*, 2017, **46**, 6816–6854.

9 C. Zhong, Y. Deng, W. Hu, J. Qiao, L. Zhang and J. Zhang, *Chem. Soc. Rev.*, 2015, **44**, 7484–7539.

10 S. Tabata, Y. Isshiki and M. Watanabe, *J. Electrochem. Soc.*, 2008, **155**, K42–K42.

11 F. Wang, X. Wang, Z. Chang, X. Wu, X. Liu, L. Fu, Y. Zhu, Y. Wu and W. Huang, *Adv. Mater.*, 2015, **27**, 6962–6968.

12 F. Wang, C. Wang, Y. Zhao, Z. Liu, Z. Chang, L. Fu, Y. Zhu, Y. Wu and D. Zhao, *Small*, 2016, **12**, 6207–6213.